

# Phase transformations in a Cu–35 at.% Mn–25 at.% Al alloy

S.Y. Yang, T.F. Liu\*

Department of Materials Science and Engineering, National Chiao Tung University, Hsinchu 300, Taiwan, ROC

Received 10 August 2005; accepted 1 September 2005

Available online 13 October 2005

## Abstract

The phase transformations in the Cu–35 at.% Mn–25 at.% Al alloy have been investigated by means of transmission electron microscopy (TEM) and energy-dispersive X-ray spectrometry (EDS). In as-quenched condition, the microstructure of the alloy was a mixture of (L<sub>21</sub> + B<sub>2</sub> + L-J) phases. This is different from that observed by previous workers in the Cu<sub>3-x</sub>Mn<sub>x</sub>Al alloys with  $x \leq 1.0$ . When the as-quenched alloy was aged at 460 °C for short times,  $\gamma$ -brass precipitates started to occur at anti-phase boundaries (APBs). After prolonged aging at 460 °C, the  $\gamma$ -brass precipitates grew and  $\beta$ -Mn precipitates were formed at the regions contiguous to the  $\gamma$ -brass precipitates. The coexistence of ( $\gamma$ -brass +  $\beta$ -Mn) has never been observed by previous workers in Cu–Mn–Al alloy systems before.

© 2005 Elsevier B.V. All rights reserved.

**Keywords:** Cu–Mn–Al alloy;  $\gamma$ -Brass; Anti-phase boundary;  $\beta$ -Mn

## 1. Introduction

In previous studies, it is seen that when the Cu<sub>3-x</sub>Mn<sub>x</sub>Al alloys with  $0.5 \leq x \leq 0.8$  were solution-treated in single  $\beta$  phase (disordered body-centered cubic) region and then quenched rapidly, a  $\beta \rightarrow B_2 \rightarrow D0_3 + L_{21}$  phase transition occurred during quenching [1]; as the Mn content in the Cu<sub>3-x</sub>Mn<sub>x</sub>Al alloy was increased to 25 at.% ( $x = 1$ ), the as-quenched microstructure of the Cu<sub>2</sub>MnAl alloy became a single L<sub>21</sub> phase [1–4]. When the Cu<sub>3-x</sub>Mn<sub>x</sub>Al alloys with  $0.5 \leq x \leq 0.8$  were aged at 300 °C or below for longer times, fine precipitates were observed to appear within the (D0<sub>3</sub> + L<sub>21</sub>) matrix [1]. The crystal structure of the fine precipitates was determined to be of L1<sub>0</sub> having lattice parameters  $a = 0.424$  nm,  $b = 0.297$  nm and  $c = 0.424$  nm [1]. In addition, three kinds of precipitates, namely,  $\gamma$ -brass (D8<sub>3</sub>),  $\beta$ -Mn (A13) and T-Cu<sub>3</sub>Mn<sub>2</sub>Al (C15) were reported to form in the Cu<sub>2</sub>MnAl alloy after being aged at temperatures ranging from 350 to 650 °C [2–4]. It is interesting to note that although the  $\beta$ -Mn precipitate was always found in the aged Cu<sub>2</sub>MnAl alloy, we are aware of only one article concerning the orientation relationship between the  $\beta$ -Mn and matrix [4]. In 1987, Kozubski et al. reported that both the morphology of the  $\beta$ -Mn precipitates and the orientation relationship between the

$\beta$ -Mn and L<sub>21</sub> matrix would vary with the aging temperature [4].

Recently, we have performed TEM investigations on the phase transformations of Cu<sub>2.2</sub>Mn<sub>0.8</sub>Al and Cu<sub>2</sub>MnAl alloys [5,6]. Consequently, we found that the fine precipitates formed in the Cu<sub>2.2</sub>Mn<sub>0.8</sub>Al alloy aged at 300 °C should belong to the L-J phase, rather than L1<sub>0</sub> phase [5]. The L-J phase has an orthorhombic structure with lattice parameters  $a = 0.413$  nm,  $b = 0.254$  nm and  $c = 0.728$  nm, which was firstly identified by the present workers. In addition, TEM examinations indicated that when the Cu<sub>2</sub>MnAl alloy was aged at temperatures ranging from 460 to 560 °C, the morphology of the  $\beta$ -Mn precipitates would change with the different aging temperature; however, in spite of the morphology change the same orientation relationship between the  $\beta$ -Mn and the L<sub>21</sub> matrix was maintained. This result is different from that reported by Kozubski et al. [4]. However, to date, all of the examinations were focused on the Cu<sub>3-x</sub>Mn<sub>x</sub>Al alloys with  $x \leq 1.0$ . Little information was available concerning the microstructural developments of the Cu<sub>3-x</sub>Mn<sub>x</sub>Al alloys containing higher Mn content. Therefore, the purpose of this work is an attempt to study the phase transformations in the Cu–35 at.% Mn–25 at.% Al alloy.

## 2. Experimental procedure

The alloy, Cu–35 at.% Mn–25 at.% Al, was prepared in a vacuum induction furnace by using 99.9% Cu, 99.9% Mn and 99.9% Al. The melt was chill

\* Corresponding author. Tel.: +886 3 573 1675; fax: +886 3 572 8504.  
E-mail address: tfliu@cc.nctu.edu.tw (T.F. Liu).

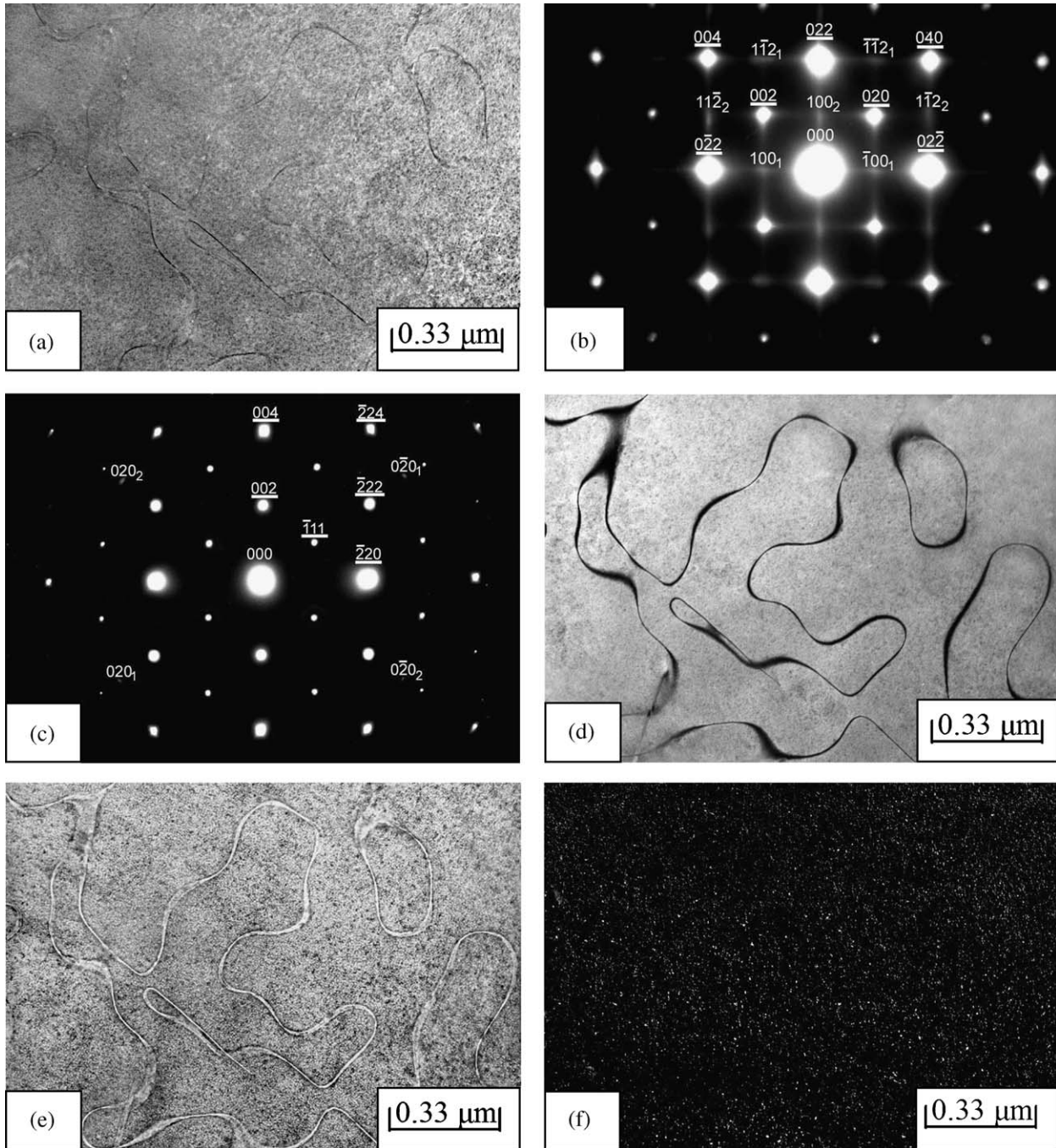


Fig. 1. Electron micrographs of the as-quenched alloy: (a) BF; (b) and (c) two SADPs. The zone axes of the  $L2_1$  phase are (b)  $[1\ 1\ 0]$  and (c)  $[1\ 1\ 0]$ , respectively ( $hkl = L2_1$ ,  $hkl_{1,2} = L\text{-}J$  phase, 1: variant 1; 2: variant 2); (d) and (e)  $(\bar{1}\ 1\ 1)$  and  $(0\ 0\ 2)$   $L2_1$  DF, respectively; (f)  $(0\ \bar{2}\ 0)$   $L\text{-}J$  DF.

cast into a 30 mm  $\times$  50 mm  $\times$  200 mm copper mold. After being homogenized at 900 °C for 72 h, the ingot was sectioned into 2.0-mm thick slices. These slices were subsequently solution-treated at 850 °C for 1 h and then quenched into room-temperature water rapidly. The aging process was performed at 460 °C for various times in a vacuum heat-treated furnace and then quenched rapidly.

TEM specimens were prepared by means of a double-jet electropolisher with an electrolyte of 70% methanol and 30% nitric acid. The polishing temperature was kept in the range from  $-30$  to  $-15$  °C, and the current density was kept in the range from  $3.0 \times 10^4$  to  $4.0 \times 10^4$  A/m<sup>2</sup>. Electron microscopy was performed on a JEOL JEM-2000FX scanning transmission electron micro-

scope operating at 200 kV. This microscope was equipped with a Link ISIS 300 energy-dispersive X-ray spectrometer (EDS) for chemical analysis. Quantitative analyses of elemental concentrations for Cu, Mn and Al were made with the aid of a Cliff-Lorimer Ratio Thin Section method.

### 3. Results

Fig. 1(a) shows a bright-field (BF) electron micrograph of the as-quenched alloy. Fig. 1(b) and (c) are two selected-area diffrac-



tion patterns (SADPs) of the as-quenched alloy. When compared with our previous studies in the  $\text{Cu}_{2.2}\text{Mn}_{0.8}\text{Al}$  and  $\text{Cu}_2\text{MnAl}$  alloys [5,6], it is found in these SADPs that the brighter and well-arranged reflection spots are of the ordered  $\text{L}_{21}$  phase and the extra spots with streaks are of the L-J phase with two variants. Although the brighter and well-arranged reflection spots could be analyzed as a single  $\text{L}_{21}$  phase, the  $\text{L}_{21}$  reciprocal lattices contain all the B2-type reflections [7,8]. Therefore, in order to decide whether the ordered B2-type phase coexists with the  $\text{L}_{21}$  phase, both electron diffraction method and dark-field technique were performed. In our previous study [6], it was found that the intensity of the  $(\bar{1}11)$  and  $(002)$  reflection spots of a single  $\text{L}_{21}$  phase should be almost equivalent. However, it is clearly seen in Fig. 1(c) that the  $(002)$  and  $(\bar{2}22)$  reflection spots are much stronger than the  $(\bar{1}11)$  reflection spot. Therefore, it is strongly suggested that the  $(002)$  and  $(\bar{2}22)$  reflection spots should derive from not only  $\text{L}_{21}$  phase but also the B2 phase, since the  $(\bar{1}11)$  reflection spot comes from the  $\text{L}_{21}$  phase only; while the  $(002)$  and  $(\bar{2}22)$  reflection spots can come from both the  $\text{L}_{21}$  and B2 phases (the  $(002)$  and  $(\bar{2}22)$   $\text{L}_{21}$  reflection spots are equal to the  $(001)$  and  $(\bar{1}11)$  B2 reflection spots, respectively). Fig. 1(d) and (e) are  $(\bar{1}11)$  and  $(002)$   $\text{L}_{21}$  dark-field (DF) electron micrographs of the as-quenched alloy. It is obviously seen that the bright region in the  $(002)$  DF image is much more than that in the  $(\bar{1}11)$  DF image. This demonstrates that both B2 and  $\text{L}_{21}$  phases are present, rather than single  $\text{L}_{21}$  phase; otherwise these two DF images should be morphologically identical. Fig. 1(f) is a  $(0\bar{2}0_1)$  L-J DF electron micrograph, revealing the presence of fine L-J precipitates. Accordingly, it is concluded that the microstructure of the alloy in the as-quenched condition was a mixture of ( $\text{L}_{21} + \text{B}_2 + \text{L-J}$ ) phases.

When the as-quenched alloy was aged at  $460^\circ\text{C}$  for less than 10 min, the sizes of both the B2 and L-J phases existing within the  $\text{L}_{21}$  matrix increased and the microstructure of the alloy was still the mixture of ( $\text{L}_{21} + \text{B}_2 + \text{L-J}$ ) phases. An example is shown in Fig. 2. However, after prolonged aging at the same temperature, heterogeneous precipitation started to occur at the APBs, as illustrated in Fig. 3(a). Fig. 3(b) is an SADP taken from an area including the precipitate marked as “R” in Fig. 3(a) and its surrounding matrix. Based on the analyses of the diffraction pattern, it is confirmed that the heterogeneously precipitated phase is  $\gamma$ -brass and the orientation relationship between the  $\gamma$ -brass and the  $\text{L}_{21}$  matrix was determined to be cubic to cubic. This is similar to that reported by previous workers in the aged  $\text{Cu}_2\text{MnAl}$  alloy [4]. With continued aging at  $460^\circ\text{C}$ , the  $\gamma$ -brass precipitates grew and another type of precipitates started to occur at the regions contiguous to the  $\gamma$ -brass precipitates, as shown in Fig. 4(a). Fig. 4(b), an SADP taken from the precipitate marked as “B” in Fig. 4(a), indicates that the new type of precipitate was  $\beta$ -Mn with lattice parameter  $a = 0.641 \text{ nm}$  [6]. Fig. 4(c) is an SADP taken from an area covering two precipitates marked as “R” and “B” in Fig. 4(a), indicating that the orientation relationship between the  $\gamma$ -brass and  $\beta$ -Mn was  $(001)_{\gamma\text{-brass}} // (012)_{\beta\text{-Mn}}$  and  $(011)_{\gamma\text{-brass}} // (031)_{\beta\text{-Mn}}$ . With the subsequent aging at  $460^\circ\text{C}$ , the precipitation of ( $\gamma$ -brass +  $\beta$ -Mn) would tend toward the inside of the  $\text{L}_{21}$  matrix, as illustrated in Fig. 5. It is thus anticipated that the microstructure of the alloy

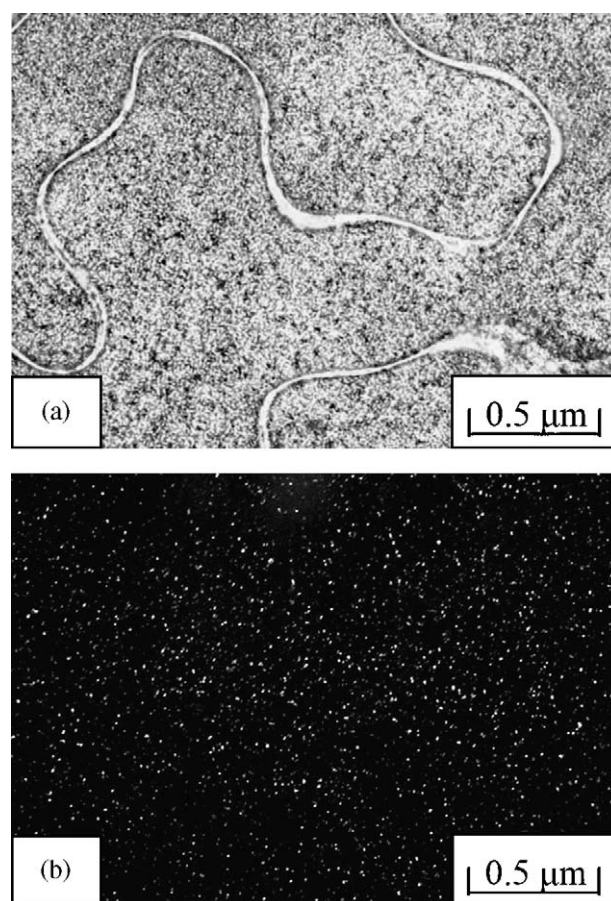


Fig. 2. Electron micrographs of the alloy aged at  $460^\circ\text{C}$  for 10 min: (a)  $(002)$   $\text{L}_{21}$  DF; (b)  $(0\bar{2}0_1)$  L-J DF.

in the equilibrium stage at  $460^\circ\text{C}$  was a mixture of ( $\gamma$ -brass +  $\beta$ -Mn).

#### 4. Discussion

That the B2 phase could be detected in the as-quenched or aged at  $460^\circ\text{C}$  alloy is a remarkable feature in the present study. This result is different from that examined by previous workers in the  $\text{Cu}_{3-x}\text{Mn}_x\text{Al}$  alloys with  $0.5 \leq x \leq 1.0$  [1–4], in which they reported that the as-quenched microstructure of the  $\text{Cu}_{3-x}\text{Mn}_x\text{Al}$  alloys with  $0.5 \leq x \leq 0.8$  was the ( $\text{D}0_3 + \text{L}_{21}$ ) phases, and that of the  $\text{Cu}_2\text{MnAl}$  alloy was the  $\text{L}_{21}$  phase; and the B2 phase could exist only at temperatures above  $600^\circ\text{C}$ . Compared to the previous studies [1–4], it is clear that besides containing higher Mn content, the chemical composition of the present alloy is similar to that of the  $\text{Cu}_{3-x}\text{Mn}_x\text{Al}$  alloys with  $0.5 \leq x \leq 1.0$ . Therefore, it is reasonable to expect that the addition of the higher Mn content in the  $\text{Cu}_{3-x}\text{Mn}_x\text{Al}$  alloys would pronouncedly enhance the formation of the B2 phase. However, the reason why the higher addition of Mn could lead to this result is unclear.

A second important feature of the present study is that when the alloy was aged at  $460^\circ\text{C}$  for moderate times, the  $\beta$ -Mn precipitates started to occur at the regions contiguous to the  $\gamma$ -brass precipitates. This precipitation behavior has never been

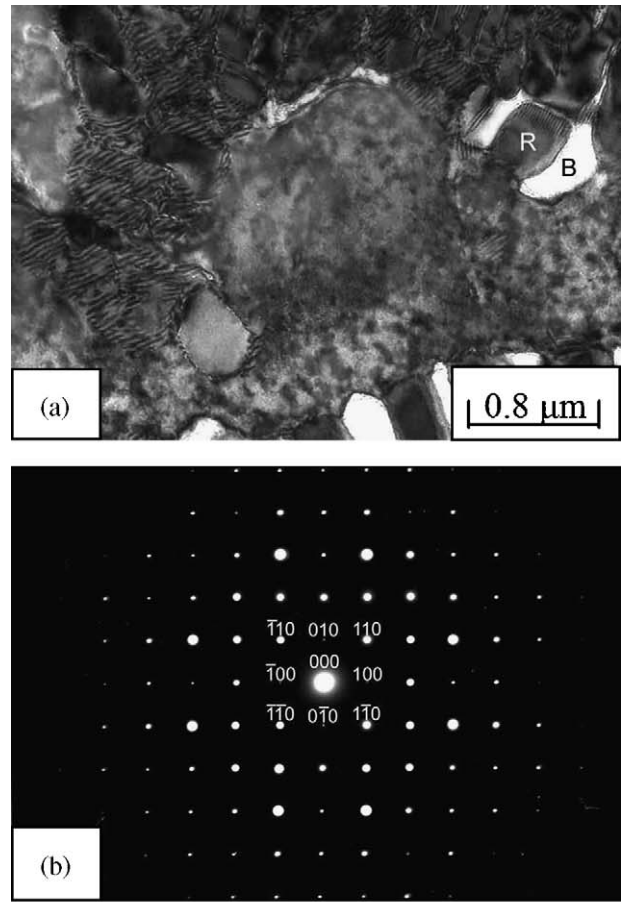
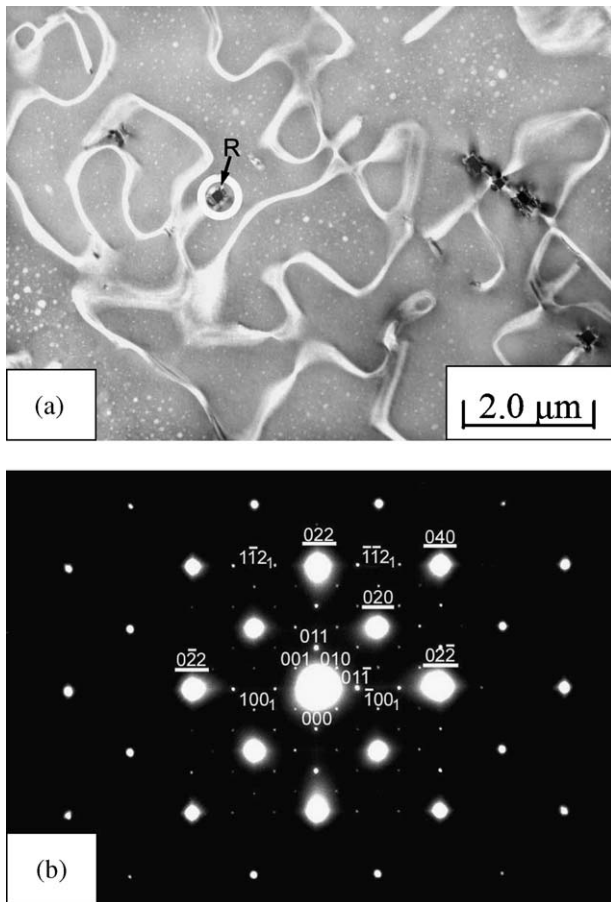


Fig. 3. Electron micrographs of the alloy aged at 460 °C for 30 min: (a) (002)  $L2_1$  DF; (b) an SADP. The zone axis of the  $L2_1$  phase is  $[1\ 0\ 0]$  ( $hkl = L2_1$ ,  $hkl = \gamma$ -brass).

observed by previous workers in the aged  $\text{Cu}_2\text{MnAl}$  alloy [3,4], in which they found that when the  $\text{Cu}_2\text{MnAl}$  alloy was aged at temperatures ranging from 350 to 650 °C, the  $\gamma$ -brass and  $\beta$ -Mn precipitates were formed separately at the grain boundaries or on other structural defects. In order to clarify this difference, an STEM-EDS study was undertaken. Fig. 6(a)–(c) represents three typical EDS spectra taken from the as-quenched alloy and the  $\gamma$ -brass as well as the  $\beta$ -Mn precipitates in the alloy aged at 460 °C for 6 h, respectively. The average concentrations of alloying elements obtained by analyzing a number of EDS spectra of each phase are listed in Table 1. It is clearly seen in Table 1 that the concentration of Mn in the  $\gamma$ -brass is only about 2.25 at.%, which is much less than that in the as-quenched alloy. It is thus expected that along with the growth of the  $\gamma$ -brass precipitates,

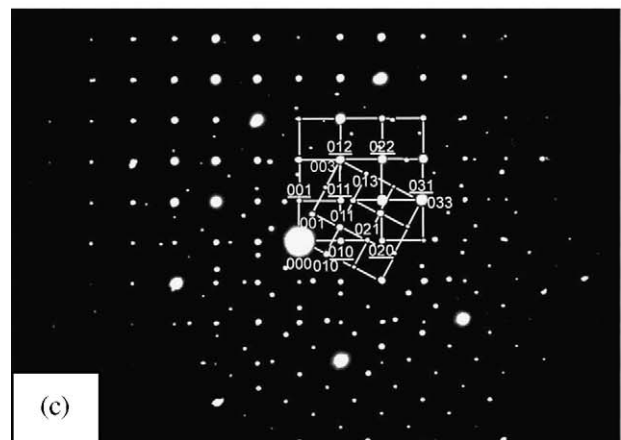


Fig. 4. Electron micrographs of the alloy aged at 460 °C for 6 h: (a) BF; (b) an SADP. The zone axis of the  $\beta$ -Mn is  $[0\ 0\ 1]$ . (c) An SADP. The zone axes of the  $\beta$ -Mn and the  $\gamma$ -brass is  $[1\ 0\ 0]$  and  $[1\ 0\ 0]$ , respectively ( $hkl = \beta$ -Mn,  $hkl = \gamma$ -brass).

Table 1  
Chemical compositions of the phases revealed by energy-dispersive X-ray spectrometer (EDS)

Heat treatment	Phase	Chemical compositions (at.%)		
		Cu	Mn	Al
As-quenched		39.81	35.11	25.08
460 °C, 6 h	$\gamma$ -Brass	67.63	2.25	30.12
460 °C, 6 h	$\beta$ -Mn	11.99	67.97	20.04

the surrounding regions would be enriched in Mn. In Cu–Mn phase diagram [9], it is clearly seen that the  $\beta$ -Mn phase could exist only when the Mn content was greater than 75 at.% and the temperature was in the range from 707 to 1100 °C; whereas the  $\beta$ -Mn phase region was pronouncedly expanded to below 427 °C with  $61 \leq \text{Mn} \leq 90$  at.% and  $10 \leq \text{Al} \leq 39$  at.% in Al–Mn binary alloys [10]. Therefore, it is reasonable to propose that at lower temperature, the concentrations of both Al and Mn would be the predominant factor for the formation of the  $\beta$ -Mn precipitates.

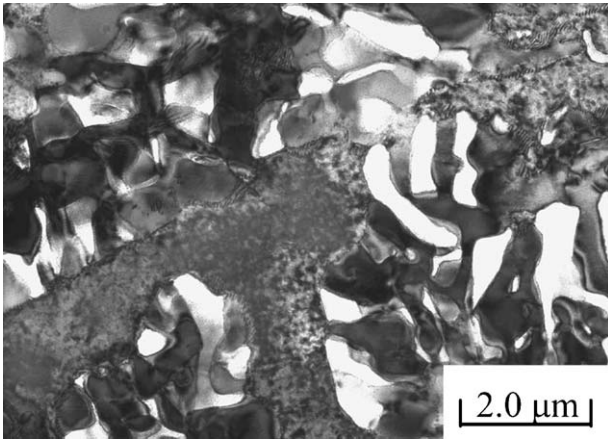


Fig. 5. BF electron micrograph of the alloy aged at 460 °C for 12 h.

In Table 1, it is obvious that the concentrations of both Al and Mn in the  $\beta$ -Mn precipitate are located within the composition range of the  $\beta$ -Mn phase region in the Al–Mn binary alloys. Therefore, the coexistence of ( $\gamma$ -brass +  $\beta$ -Mn) is expected to occur. In contrast to the observations in the present alloy, although the Mn-lack  $\gamma$ -brass precipitates were also observed to occur in

the aged Cu<sub>2</sub>MnAl alloy, no evidence of the  $\beta$ -Mn precipitates could be detected at the regions contiguous to the  $\gamma$ -brass precipitates [4,6]. The reason is probably that along with the growth of  $\gamma$ -brass precipitates, the Mn concentration at the regions surrounding the  $\gamma$ -brass may not be sufficient to cause the formation of the  $\beta$ -Mn precipitates.

Finally, it is worthwhile to note that during the early stage of isothermal aging at 460 °C, the  $\gamma$ -brass precipitates have occurred preferentially at APBs. This feature is similar to that observed by other workers in an aged Cu–14.6 wt.% Al–1.95 wt.% Ni alloy [11].

## 5. Conclusion

The as-quenched microstructure of the Cu–35 at.% Mn–25 at.% Al alloy was a mixture of ( $L2_1 + B2 + L$ -J) phases. When the as-quenched alloy was aged at 460 °C for moderate times,  $\beta$ -Mn precipitates were formed at the regions contiguous to the  $\gamma$ -brass precipitates. The orientation relationship between the  $\gamma$ -brass and  $\beta$ -Mn was  $(001)_{\gamma\text{-brass}} // (012)_{\beta\text{-Mn}}$  and  $(011)_{\gamma\text{-brass}} // (031)_{\beta\text{-Mn}}$ . The coexistence of ( $\gamma$ -brass +  $\beta$ -Mn) has never been observed by previous workers in Cu–Mn–Al alloy systems before.

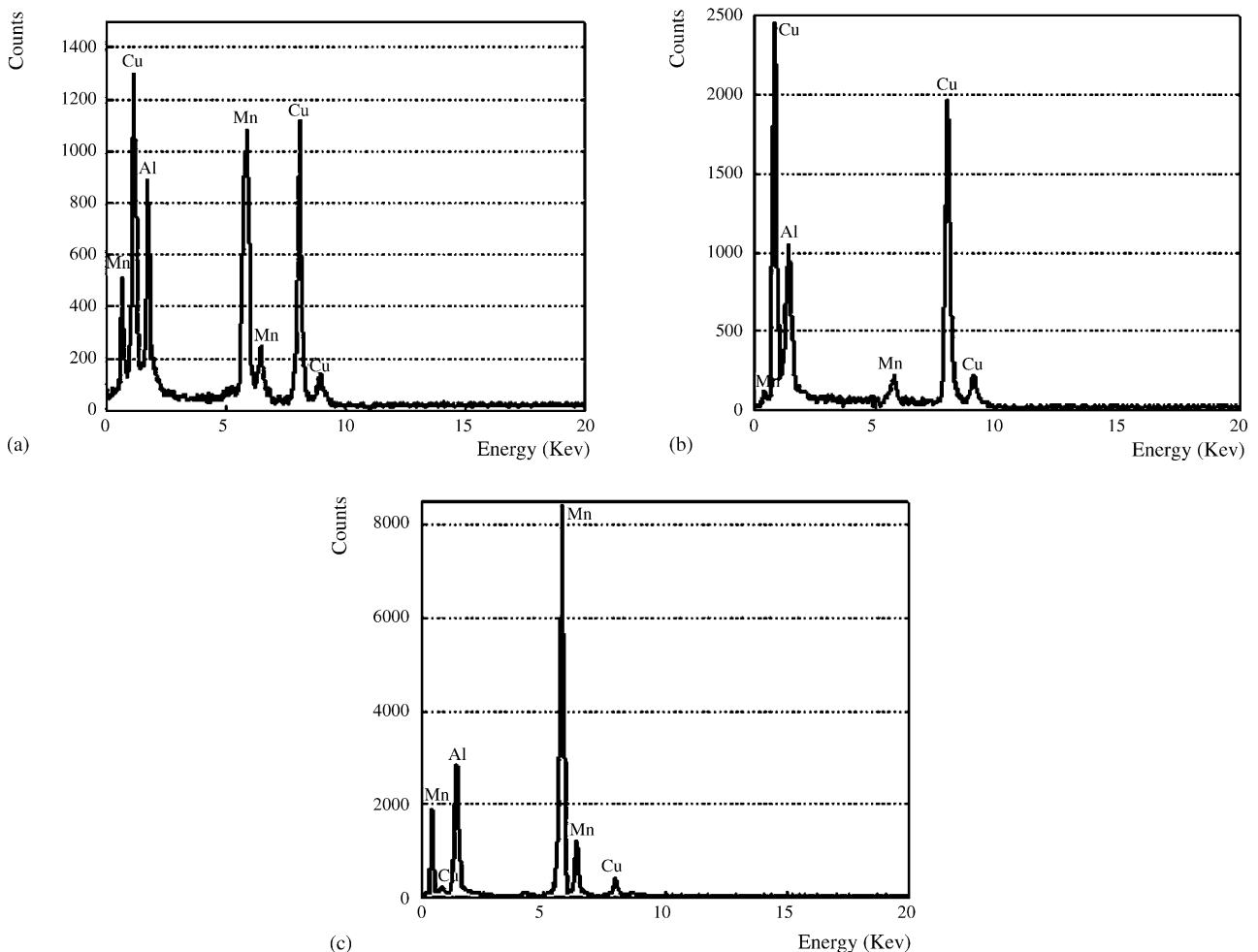


Fig. 6. Three typical EDS spectra obtained from (a) as-quenched alloy, (b) a  $\gamma$ -brass precipitate as well as (c) a  $\beta$ -Mn precipitate in the alloy aged at 460 °C for 6 h.

## Acknowledgments

The authors are pleased to acknowledge the financial support of this research by the National Science Council, Republic of China under Grant NSC93-2216-E009-016. He is also grateful to M.H. Lin for typing.

## References

- [1] M. Bouchard, G. Thomas, *Acta Metall.* 23 (1975) 1485–1500.
- [2] R. Kainuma, N. Satoh, X.J. Liu, I. Ohnuma, K. Ishida, *J. Alloys Compd.* 266 (1998) 191–200.
- [3] R. Kozubski, J. Soltys, *J. Mater. Sci.* 18 (1983) 1689–1697.
- [4] R. Kozubski, J. Soltys, J. Dutkiewicz, J. Morgiel, *J. Mater. Sci.* 22 (1987) 3843–3846.
- [5] S.C. Jeng, T.F. Liu, *Metall. Mater. Trans. A* 26 (1995) 1353–1365.
- [6] K.C. Chu, T.F. Liu, *Metall. Mater. Trans. A* 30 (1999) 1705–1716.
- [7] T.F. Liu, G.C. Uen, C.Y. Chao, Y.L. Lin, C.C. Wu, *Metall. Trans. A* 22 (1991) 1407–1415.
- [8] C.C. Wu, J.S. Chou, T.F. Liu, *Metall. Trans. A* 22 (1991) 2265–2276.
- [9] F.A. Shunk, in: Thaddeus B. Massalski (Ed.), *Binary Alloy Phase Diagrams*, American Society for Metals, Metals Park, Ohio, 1990, pp. 1435–1436.
- [10] X.J. Liu, I. Ohnuma, R. Kainuma, K. Ishida, *J. Phase Equilib.* 20 (1999) 45–56.
- [11] P.R. Swann, *Phil. Mag.* 14 (1966) 461–471.